



Article

Wear Model of a Mechanical Seal Based on Piecewise Fractal Theory

Xingya Ni , Jianjun Sun ^{*}, Chenbo Ma and Yuyan Zhang

School of Mechanical and Electronic Engineering, Nanjing Forestry University, Nanjing 210037, China

^{*} Correspondence: sunjianjun@njfu.edu.cn

Abstract: In this research, a model is proposed using piecewise fractal theory that considers abrasive and adhesive wear. The model demonstrated improved wear computation accuracy of a contact mechanical seal end face. The validity of the model was established by comparing the simulation results with experimental data and the conventional MB and Archard models. The loading effect and surface morphology parameters involved in wear were also investigated. Results show that severe wear occurs with increasing load ratio, large fractal dimensions, and a higher scale coefficient of the surface morphology. The findings offer a novel method for precisely calculating and projecting the amount of wear of a contact mechanical seal and predicting its wear behavior.

Keywords: mechanical seal; adhesive wear; abrasive wear; fractal theory

1. Introduction

The demand for mechanical seals is growing at a rapid pace due to the increased use of mechanical and electromechanical devices. Numerous studies have been reported in the published literature that focus on the design of mechanical seals and their performance. For instance, Mayer [1] studied changes in the friction coefficients of various materials by using water and diesel and developed the corresponding wear curves. In the study, end-face friction of mechanical seals was investigated in various forms, such as boundary friction, fluid friction, and mixed friction.

Gu [2] investigated the wear of mechanical seal end faces and developed a formula for calculating the wear of seals. Wei et al. [3] studied working conditions and proposed a wear model of the mechanical seal end face. They studied the relationship between material characteristics and mechanical seal end face wear.

The working environment of a contact face seal exists in a mixed lubrication state. The inevitable face wear increases the leakage rate and seal failure. Many accidents have been reported in the literature due to the failure of mechanical seals. For example, the primary circulation system of a heavy water reactor nuclear power plant uses a shaft seal pump, and its failure causes a shutdown of the complete reactor for emergency maintenance, which results in great financial loss. Wei [4] analyzed the macromorphology, micromorphology, and operation history of the failed seal ring, and found that failure occurred due to the compression of the moving ring spring that was large during the initial installation, and the dry friction of the moving and stationary rings produced initial thermal cracks. Subsequently, the thermal cracks expanded under the action of alternating load, and the fragments at the intersection fell off, resulting in abrasive wear of the stationary ring.

Several numerical models have been proposed for mechanical seals. Presently, the widely used wear quantitative model is based on Archard's adhesive wear [5]. The model is based on the experiment and solely takes into account the measured load, wear length, hardness, and wear coefficient. The formula is simple to understand and compute. Gu et al. [6] used Archard's wear theory and developed the quantitative expression of the worn form of a contact mechanical seal by introducing the wear coefficient. Wei et al. [7] worked on



Citation: Ni, X.; Sun, J.; Ma, C.; Zhang, Y. Wear Model of a Mechanical Seal Based on Piecewise Fractal Theory. *Fractal Fract.* **2023**, *7*, 251. <https://doi.org/10.3390/fractalfract7030251>

Academic Editor: Bruce Henry

Received: 25 January 2023

Revised: 4 March 2023

Accepted: 6 March 2023

Published: 10 March 2023



Copyright: © 2023 by the authors. Licensee MDPI, Basel, Switzerland. This article is an open access article distributed under the terms and conditions of the Creative Commons Attribution (CC BY) license (<https://creativecommons.org/licenses/by/4.0/>).

Archard's adhesive wear theory and explained the relationship between end face fractal parameters and wear rate to predict the wear of a soft sealing surface.

According to certain researchers, mechanical seals perform best in specific environments and structural configurations. Adhesive wear is more readily produced at higher wear process temperatures and on low-hardness material. A material is more susceptible to abrasive wear the rougher its surface is. When a mechanical seal is operating at its best, its service life and sealing performance can be improved. The friction and lubrication between the end face of a mechanical seal change with a change of state parameters. A dynamic model can be established to simulate the parameter sensitivity, the wear amount, and the life prediction of the seal face.

In this study, three factors are studied that greatly affect the wear of an end face seal, including speed, load, and temperature. The wear prediction model was developed considering the experimental results. By establishing a segmented fractal model, the wear process was subdivided to improve the calculation accuracy of wear and to predict the life of the end face.

2. Wear Calculation Model Based on Piecewise Fractal Theory

As shown in Figure 1, when dynamic and static rings contact each other, first, they squeeze at the highest point and then gradually fit on the middle contact surface. This process is not fully completed during the installation phase because the contact surface takes time to gradually shape during its actual operation, which is called running in.

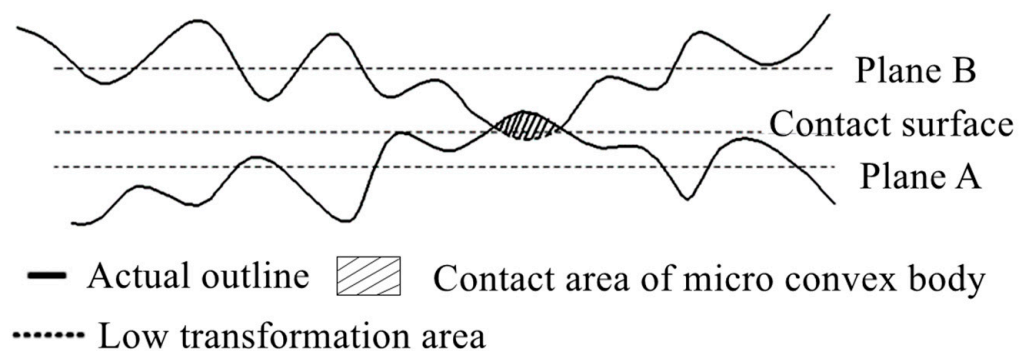


Figure 1. Contact area of a microconvex body.

By analyzing the wear mechanism of the end face of the contact mechanical seal and following the change law of wear rate, the wear process is divided into a running-in period and a stable period. Normally, the wear rate in the running-in period is high, it decreases with time, and the main wear form is abrasive wear. The wear rate in the stable period is low, which changes little with time, and the main wear form is adhesive wear. Based on the above wear mechanism and fractal theory, a segmented fractal model with two in contact rough surfaces was constructed:

$$h = \begin{cases} q_1 t_1 K_s (F - t \cdot \Delta F / t_1) / \Delta t H S + q_2 (Kv / HS) \int_0^{t_1} \sigma(t) dt & 0 \leq t \leq t_1 \\ (Kv / HS) \int_{t_1}^{t_n} \sigma(t) dt & t_1 < t \leq t_n \end{cases} \quad (1)$$

where h is the wear thickness. It is a function of time that is averaged over the position. t_1 is running in time, K_s is the abrasive wear coefficient, and $K_s = (D - 1)\phi\zeta / \pi D$. F is the load, and ΔF is the elastic force lost with time. H is the hardness of the stationary ring material, and K is the wear factor that is measured by experiment. v is the average slip velocity, $\sigma(t)$ is the function that is obtained from the polynomial model fitted in the experiment, and $\sigma(t)$ describes the stress at a specific time. q_1, q_2 are the weight coefficient values that are measured in the experiment, and $q_1 + q_2 = 1$. ζ is the probability of generating wear debris, and ϕ is the material parameter.

In Equation (1), the expression is divided into two sections. The first section is an abrasive wear model, and the second section is an improved Archard adhesive wear model.

This model is significantly different from other models that study the wear of different objects. In the modeling of tire wear, Farroni uses the ETA model to calculate the adhesive and hysteretic components of friction [8]. In the analysis of the wear of lead screw actuators, the theory of asperity contact and Archard's model of sliding wear were applied [9]. To give the wear predictions for cams, Qin and Duan adopted multibody system dynamic analysis [10]. Compared with these models, the piecewise fractal model in this paper is more targeted for the wear prediction of a contact mechanical seal. The contact mechanical seal in this research has the following characteristics:

- Ignore the influence of aging of the rubber O-ring;
- The contact surface materials are graphite and silicon carbide;
- The surface temperature is regarded as a constant temperature;
- Provide initial roughness, and the distribution of rough peaks is regular.

When the wear surface height of the stationary ring is known, the service life of the corresponding stationary ring can be estimated from the numerical model. In the proposed model, the abrasive wear model was derived from the basic M-B original model.

2.1. M–B Original Model

Contact is regarded as the contact between a rough surface and a smooth plane. Mandelbrot proposed an expression of the fractal curve function based on the Weierstrass function in 1977, which is called the Weierstrass Mandelbrot fractal function (W-M function for short) [11]. In 1991, Majumdar and Bhushan proposed a contact model based on fractal characteristics to describe the characteristics of equivalent rough surfaces [12]. It is abbreviated as the M–B model. Assuming that the rough surface is defined by the W-M function, and the deformation state of the microconvex body is related to its contact area, combined with Mandelbrot's research on island area distribution theory, a size-independent M–B contact model is proposed [13].

As shown in Figure 2, the rough surface is in contact with the smooth surface. The area distribution function of microbumps is given by:

$$n(a) = Da_1^{(D/2)} / (2a^{((D+2)/2)}) \quad (2)$$

where a is the area of the microconvex body, a_1 is the maximum microconvex area, a_c is the critical area to distinguish elastic–plastic contact, and D is the fractal dimension. Additionally, $1 < D < 2$, which can be obtained by the structure function method [14].

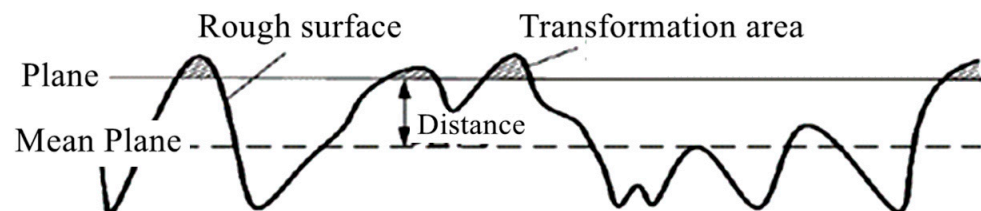


Figure 2. The contact of the rough surface and plane body.

For characterization of the rough surface, the M–B model solves the influence of sampling length and instrument resolution, but the M–B model (corresponding to contact area A) gives incorrect results and replaces the initial contour with the change of contact area A . Therefore, it can be concluded that first, the microconvex body undergoes complete plastic deformation and then elastic–plastic deformation and elastic deformation.

2.2. Contact Deformation Mechanism of the Microconvex Body

Persson et al. proposed a contact mechanics theory considering multiscale effects with the help of mathematical methods, such as fractal theory and frequency-domain transformation. Lorenz et al. verified Persson's contact mechanics model through experiments and found that the experimental data were in good agreement with theoretical data [15].

Under the action of contact load, Persson's model relies on three deformation states of the microconvex body on the rough surface, namely, elastic deformation, elastic-plastic deformation, and complete plastic deformation.

2.3. Abrasive Wear Model

At present, the abrasive wear model provides better wear calculations because it is based on the theory of regular fractals [16]. This method includes the plastic deformation wear mechanism. There are two main forms of plastic deformation wear: The first type of wear occurs when the abrasive particles are pressed into the matrix under the action of external force (due to the relative movement between the abrasive particles and the matrix), and the second type takes place when abrasive particles squeeze some materials on both sides to form furrows. Under the repeated overlapping action of abrasive particles, the uplifted parts on both sides of the furrow quickly break and form wear debris. When the abrasive particles are pressed into the matrix, they cut the matrix due to tangential force and also cut a furrow along the sliding direction. The volume of the furrow is the volume of spalling. The formation of the furrow in plastic deformation wear is related to the depth of the abrasive particles which are pressed into the matrix. The volume of the furrow is the wear volume $w(a)$, which can be expressed as:

$$w(a) = A(a)l = \frac{2}{\pi} G^{(D-1)} a^{((4-D)/2)} \quad (3)$$

where G is the amplitude coefficient of the fractal parameter.

When a single spherical peak of a rough surface slides a wavelength distance of L along the sliding direction, the spherical peak produces $w(a)$ volume of wear debris at the contact point. The section area of the spherical peak $A(a)$ is given by:

$$A(a) = \int_{-1/2}^{1/2} z dx = \frac{2}{\pi} G^{(D-1)} a^{((3-D)/2)} \quad (4)$$

The total volume of debris generated by all abrasive particles on the whole contact surface W is:

$$W = \int_0^{a_c} w(a)n(a)da = \frac{D}{\pi(2-D)} G^{(D-1)} a_l^{(D/2)} a_c^{(2-D)} \quad (5)$$

The area distribution function $n(a)$ of the contact point can be solved according to Equation (2) where a_l is the maximum area of the contact point, a is the area of the contact point, and a_c is the critical area to distinguish elastic-plastic contact.

The wear rate of the friction pair on the whole contact surface is:

$$V = W/\bar{l} = \frac{D-1}{\pi(2-D)} G^{(D-1)} a_l^{(D/2)} a_c^{((3-2D)/2)} \quad (6)$$

For all abrasive particles, when w -volume debris is generated, the average sliding distance of the friction pair is \bar{l} , the model of l is shown in Figure 3. In the above derivation, it is assumed that debris are generated during the sliding of abrasive particles; however, practically, only some abrasive particles generate debris. Let the probability of each abrasive particle generating debris be ζ :

$$V = \frac{D-1}{\pi(2-D)} \left(\frac{2-D}{D}\right)^{(D/2)} G^{(2-D)} A_r^{(D/2)} \phi^{\frac{3-2D}{1-D}} \zeta \quad (7)$$

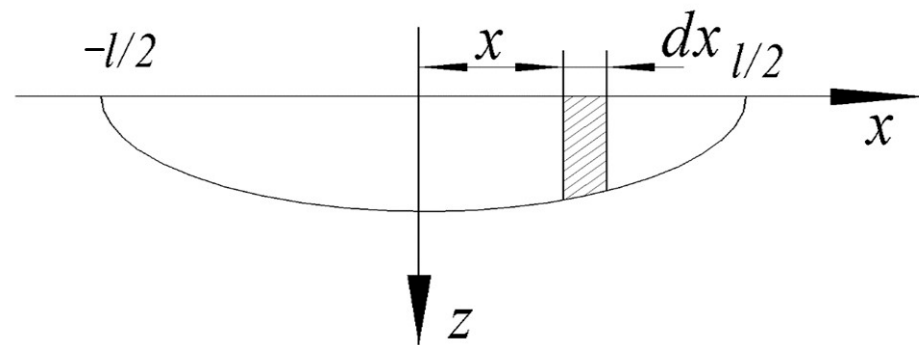


Figure 3. Contact point with wavelength l .

According to Equation (8), the wear rate of materials changes with the changes of D , G , and other parameters. Where ϕ is the material property constant, $\phi = (Q\sigma_s)/2E$. σ_s is the yield limit of the material, E is the elastic modulus, and Q is the ratio of hardness H to the yield limit. It must be noted that the real contact area is affected by the normal load P .

2.4. Simulation Steps

The three main parameters affecting the fractal contact model include the characteristic scale G , material characteristic parameters ϕ , and fractal dimension D . In this study, the control variable method was used to evaluate these three parameters, and MATLAB was employed to simulate and analyze the model. The applied load P and actual contact area a were analyzed when any parameter changed the relationship between A_r . The simulation process is shown in the flow chart (Figure 4).

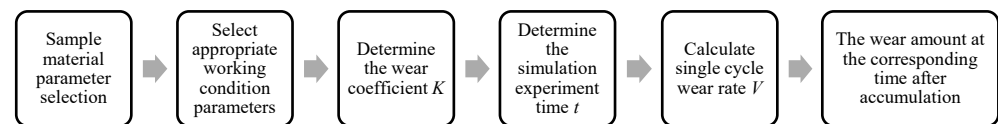


Figure 4. Simulation process flow chart.

During the entire wear process, the morphology of the end face of the mechanical seal soft ring changes dynamically; hence, the fractal parameters D and G and the wear rate are time-varying parameters. Equation (8) is a dynamic equation that explains the quantitative description of the time-varying wear characteristics of materials.

3. Data Acquisition and Wear Analysis of Mechanical Seal

This section may be divided into subheadings. It should provide a concise and precise description of the experimental results, their interpretation, as well as the experimental conclusions that can be drawn. In this study, the mechanical seal face parameters were obtained by experiments. Experimental materials included dynamic and static rings, as Figure 5a shown. The accelerated test was conducted on MMU-2 high-speed friction and wear testing machines, as shown in Figure 5b. The static ring was weighed with a PL403 precision electronic balance before and after each test. The surface morphology was developed by an LI-3 contact surface profilometer, and the static ring was heated with a 101A-1 electric blast furnace to avoid the influence of lubricating oil. The average thickness of the end face was measured with an electronic digital micrometer before and after the experiment.

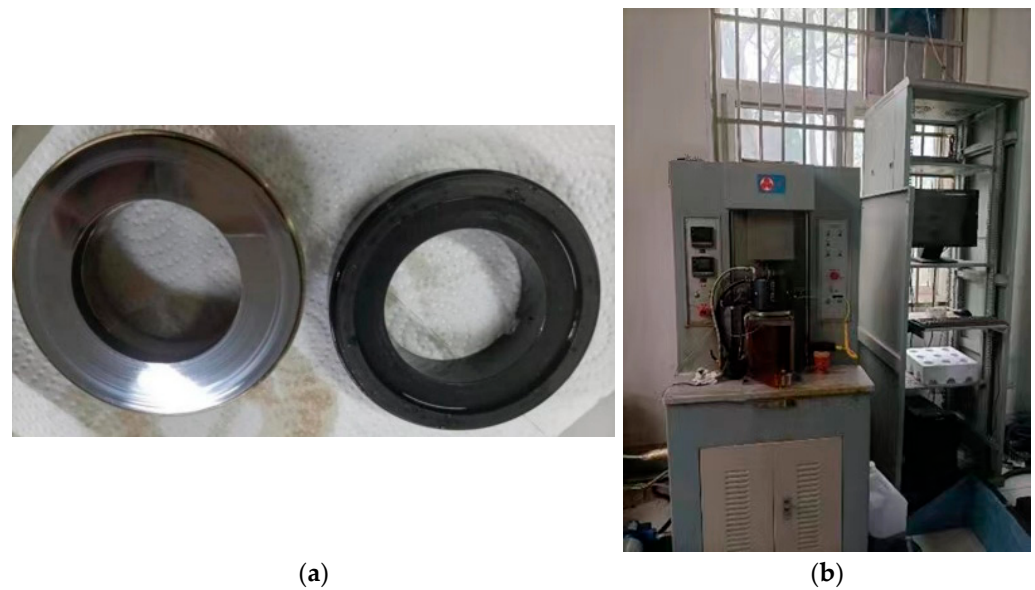


Figure 5. Test object and equipment. (a) Dynamic and static rings for experiment. (b) The testing machine.

In the experiments, a hard rotating ring was used (an upper sample rotating) around the rotating axis, and a fixed ring was used at the lower sample and fixed in the fixture. The samples were designed according to the BGMFL85 mechanical seal. Considering the load, speed, and temperature, the friction characteristics of the friction pair were estimated. The single-factor method was adopted to change the load, speed, and lubricating medium temperature of the sealing surface.

In this experiment, the inner and outer diameters of the moving ring were 60 mm and 86 mm, and the initial surface roughness was estimated Ra as 0.02. The inner and outer diameters of the stationary ring were 72 mm and 84 mm, and the initial surface roughness Ra was evaluated as 0.4. Other parameter settings on the experimental trial are delivered in Table 1.

Table 1. Experimental parameters.

Time/h	5	10	15	20	30
Instrument	MMU-2 high-speed end face friction and wear testing machine				
Moving ring	Cemented carbide YG8 (left in the picture)				
Stationary ring	Carbon graphite M106k				
Rotating speed/RPM	2000				
Load/N	600				
Temperature/°C	150				
Lubricating medium	SH710 multifunctional phenylmethyl silicone oil				

In this experiment, the testing machine was controlled through software, and the wear of impregnated graphite stationary rings was studied under different working conditions. After measuring the initial thickness of the stationary ring with an electronic micrometer, the testing machine was started and continuously run for 30 h, then the thickness of the stationary ring was measured again. Before estimating friction, the machine started to heat the oil tank to attain a predetermined temperature value. The amount of wear was calculated by an electronic micrometer, and the experimental data were studied to analyze the influence of speed, temperature, load on the wear amount and the failure form of the BGMFL85 series bellows mechanical seal. The results of the graphite ring response surface experiment were considered the benchmark for comparison. By using the response surface software, the wear function of the graphite ring was fitted, the service life of the graphite ring under specific working conditions was predicted, and the end face wear factor in the contact mechanical seal was obtained. The experimental data were compared with

the published data, and the advantages and disadvantages were identified to find the optimization scheme. The experimental data table is given in Table 2.

Table 2. Experimental data.

Rotating Speed/rpm	Oil Temperature/K	Load/N	Time/h	5	10	15	20	30
2000	423	600	Interface medium temperature/K	459	482	472	439	438
			Friction torque/N·m	2.6	3.6	3.0	1.5	2.4
			Friction/N	66.7	92.3	76.9	38.5	61.5
			Friction coefficient	0.11	0.15	0.13	0.06	0.10
			Wear depth/mm	0.0405				
			Wear coefficient	6.81×10^{-10}				

3.1. Experimental Model Analysis

The speed, load, and temperature were taken as critical factors, affecting the wear amount (i.e., the response value). The investigation factor was set as the relationship between the three factors that affect the wear amount. The BBD (Box-Behnken Design) experimental design table is presented in Tables 3 and 4, and the results obtained by the software are shown in Table 5.

Table 3. Experimental factors and levels.

Factor	−1	0	1
A Rotating speed /rpm	1000	1500	2000
B Load/N	300	600	900
C Temperature/K	393	423	453

Table 4. The experimental results.

No.	Rotating Speed/rpm	Load/N	Temperature/K	Wear/mm
1	1000	300	423	0.021
2	2000	300	423	0.01925
3	1000	900	423	0.021
4	2000	900	423	0.0275
5	1000	600	393	0.02275
6	2000	600	393	0.0411
7	1000	600	453	0.0257
8	2000	600	453	0.0405
9	1500	300	393	0.0213
10	1500	900	393	0.0254
11	1500	300	453	0.0284
12	1500	900	453	0.0266
13	1500	600	423	0.032
14	1500	600	423	0.0391
15	1500	600	423	0.0392
16	1500	600	423	0.0393
17	1500	600	423	0.0392

Table 5. Statistical analysis of regression equation errors.

Statistical Items	Value	Statistical Items	Value
Std. Dev.	0.0046	R ²	0.8549
Mean	0.0300	Adjusted R ²	0.6684
C.V. %	15.51	Predicted R ²	−0.7465
		Model Precision	5.9072

In this study, Design-Expert software was used to process the results of the experiment [17]. After the experimental design and exporting of the experimental data, the significance of the model and the mismatch term was tested, and the correlation between various factors was compared to select the appropriate model. The variance was analyzed according to the second-order polynomial model, and significance was tested. Through in-depth analysis of the regression equation by Design-Expert, the error value of each statistical item was calculated. The results are given in Table 5.

From Table 5, it can be observed that the experimental model demonstrates good adaptability.

3.2. Analysis of Experimental Results

From the presented results, it can be observed that the maximum wear in the thirty h experiment occurred during the first two hours. This shows that the probability of failure in the early stage of equipment operation cannot be ignored. Hence, the piecewise fractal model is more practical for predicting wear.

In addition to the common planning and furrow, adhesive wear dominates during the wear mechanism. In relative motion, the polymerization force of surface molecules is less than the intermolecular force on the surface of another object, resulting in biomass transfer [18,19]. This phenomenon is called adhesive wear. The intermolecular force is called the van der Waals force. Its macroscopic manifestation shows the hardness of matter; the greater the hardness, the greater the intermolecular force. The intensity of adhesive wear transfers from low-hardness materials to high-hardness materials. When the transfer amount is enough to cover the maximum contact area, the molecular polymerization force on the contact area tends to balance, and the wear rate drops to the lowest point under this condition. Adhesive wear is also associated with solid-state welding, which refers to the welding of metal materials under static or dynamic load depending on the distance between atoms that are close to the lattice or through physical metallurgical processes, such as diffusion and recrystallization. These welding methods include cold load welding, friction welding, ultrasonic welding, explosive welding, and diffusion welding.

With an increased load, the ratio of the surface molecular distance between the two interfaces that are close to the lattice distance increases; hence, the degree of adhesive wear intensifies the amount of wear. To a certain extent, the increased load makes the wear particles deeply embedded in the surface of the soft ring. Although the depth of the wear marks is increased, it also hinders the generation of furrows. At a higher speed, the surface of the soft ring easily flakes off, thus increasing the possibility of accidental failure. If the abrasive wear is reduced through early preparation, the failure probability of the end face seal is greatly reduced.

4. Wear Calculations of Contact Mechanical Seal Considering the Piecewise Fractal Model

To illustrate the feasibility of adopting the proposed model for calculating the wear of contact mechanical seals, the results were compared with the traditional Archard model [5,20] and the M–B fractal model [12]. The simulation test conditions [21] and dynamic change of friction torque, friction coefficient, wear rate, and other parameters were noted under 3000 rpm, the end load at 400, 600, 800, 1000, and 1200 N, and the time 2, 4, 6, 8, 10 h. The inner and outer diameters of the moving ring were 50 mm and 63 mm, and the initial surface roughness was estimated at 0.02.

In this study, the values of surface topography parameters were taken from the published data. The inner and outer diameters of the stationary ring were 53 mm and 61 mm, and the initial surface roughness was noted at 0.4. N32 hydraulic oil (No. 32 antiwear hydraulic oil) was used as the lubricating medium in this experiment, and the experimental temperature was kept at 70 °C [22].

In this experiment, the hardness of static ring H was observed at 80 when $P = 600$ N, and the average wear thickness \bar{h} after 30 h was estimated at 0.0405 mm. The friction distance S was calculated as

$$S = 2000 \times 60 \times 30 \times \pi \cdot (R + r) = 3,600,000 \times 0.24492 = 881,712\text{m} \quad (8)$$

The wear coefficient K was calculated as

$$K = \frac{\bar{h}}{P} \cdot \frac{H}{S} \approx 6.8 \times 10^{-11} \quad (9)$$

Figure 6 provides the comparison of the changes in ten-hour wear for three models and the experimental values published in the literature. It can be observed that the wear amount calculated by the three models increases with time, while the increased range decreases, which is consistent with the actual operating conditions. In addition, under the same conditions, the calculation results of the three models lie within the same order of magnitude, and the wear amount calculated by the Archard model is the smallest in the early stage, while the wear amount calculated by the MB theoretical model is the minimum in the late stage. In this study, the calculation results of the segmented fractal model are close to the experimental values.

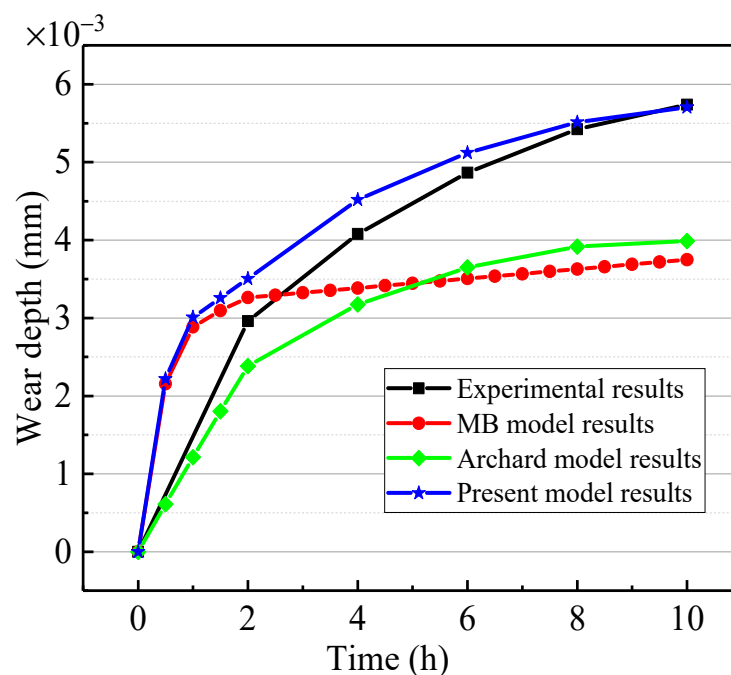


Figure 6. Comparison of different results.

5. Analysis of Wear Characteristics of Contact Mechanical Seal

For the wear of the mechanical seal interface, the contact area must also be considered in addition to a certain load and relative movement. Different contact areas correspond to different stresses, and different contact types can be identified under the same load.

5.1. Effects of Load on Sealing Surface

Numerous studies have shown that under the same operating parameters, the wear increases with the load when it is in a certain range. Figure 7 shows that the wear changes in the first 2 h, 10 h, and 20,000 h when the positive load P is 400 N, 600 N, 800 N, and 1000 N.

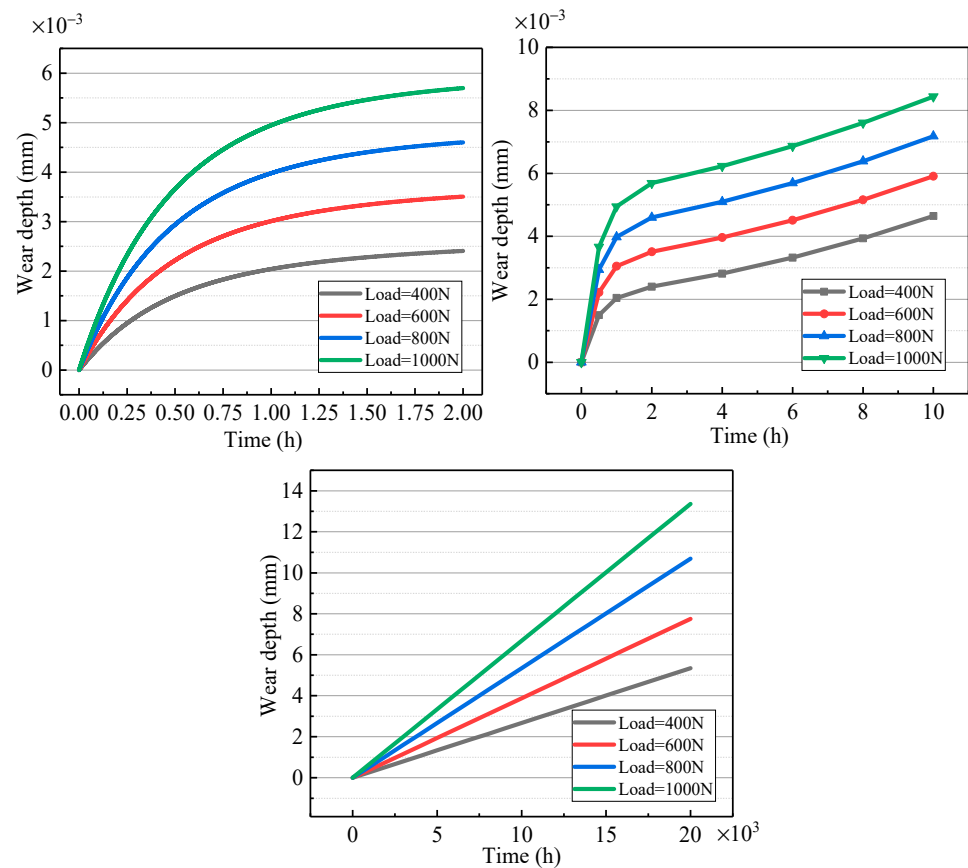


Figure 7. Wear under different load conditions (from 0 to 20,000 h).

The actual contact area on the contact surface changes with the positive load, and the contact state changes accordingly. Tomlinson's [23] research supports this explanation. Under the action of molecular activity and molecular force, the solid produces friction resistance and hinders relative sliding. Then, Bowden and Tabor established a relatively complete theory of adhesive friction through systematic experimental research and concluded that friction occurred due to the furrow effect and adhesive effect between solids [24].

Most of the published studies on friction rarely focused on the contact load between solids, and the effect of the sliding speed on the contact load distribution was not discussed until now. When the contact load changes, the actual contact area changes accordingly, which affects the calculation of the final wear. The published studies have reported the simplified formula for calculating the contact area [25]:

$$a_r = \frac{1}{\pi} \left(\frac{3p_m}{4EG^{(D-1)}l^{-D}} \right)^2 \quad (10)$$

a_r is the contact area of a single microconvex body, p_m is the average contact stress, l is the bottom diameter of the microconvex contour, $l = \left(\frac{h}{G^{D-1}} \right)^{\frac{1}{2-D}}$, and the maximum microconvex height of the hard ring and the soft ring on the rough surface are taken as $h_1 = 0.2 \mu\text{m}$ and $h_2 = 0.4 \mu\text{m}$, respectively. The equivalent rough peak height $h = 0.477 \mu\text{m}$ can be obtained from the expression $h = \sqrt{h_1^2 + h_2^2}$. This expression applies to the elastic deformation stage in which the average contact load p_m on the contact surface is less than the yield limit of the material with rough surface σ_y .

$$a_r = \frac{e^7}{\pi^3} \left(\frac{p_m}{EG^{(D-1)}l^{(-D)}} \right)^2 \quad (11)$$

Equation (10) provides the complete plastic deformation where the average contact load p_m is greater than $3\sigma_y$, and the microconvex body completely yields. For the elastic-plastic deformation, the effects of contact area, contact load during elastic deformation, elastic-plastic deformation, and complete plastic deformation were considered. The results show that the change is continuous and smooth; hence, it can be regarded as a one-dimensional linear function relationship [26].

The relationship between the actual contact area and the contact load is obtained by:

$$a_r = \begin{cases} \frac{1}{\pi} \left(\frac{3p_m}{4EG^{D-1}l^{1-D}} \right)^2 & p_m \leq \sigma_y \\ \left[(p_m - \sigma_y) \left(\frac{e^7}{\pi^3} \left(\frac{3\sigma_y}{EG^{D-1}l^{1-D}} \right)^2 - \frac{1}{\pi} \left(\frac{3\sigma_y}{EG^{D-1}l^{1-D}} \right)^2 \right) / 2\sigma_y \right] + \frac{1}{\pi} \left(\frac{3\sigma_y}{4EG^{D-1}l^{1-D}} \right)^2 & \sigma_y \leq p_m \leq 3\sigma_y \\ \frac{e^7}{\pi^3} \left(\frac{p_m}{EG^{D-1}l^{1-D}} \right)^2 & p_m \geq 3\sigma_y \end{cases} \quad (12)$$

$$A_r = 4a_r A / (\pi l^2) \quad (13)$$

where A_r is the macro real contact area, and A is the nominal contact area.

Figure 8 shows the change of real contact area with force. Figure 8a shows the relationship between the real contact area of the microconvex body and the contact force. Figure 8b shows the macroscopic analysis of actual contact area after being stressed. It can be observed that the increase in load increases the real contact area, which increases the furrow effect and adhesion effect between solids, thus increasing the wear. With the increase of the real contact area, plastic deformation increases, and the increasing trend is observed for the actual contact area; hence, the wear rate also increases.

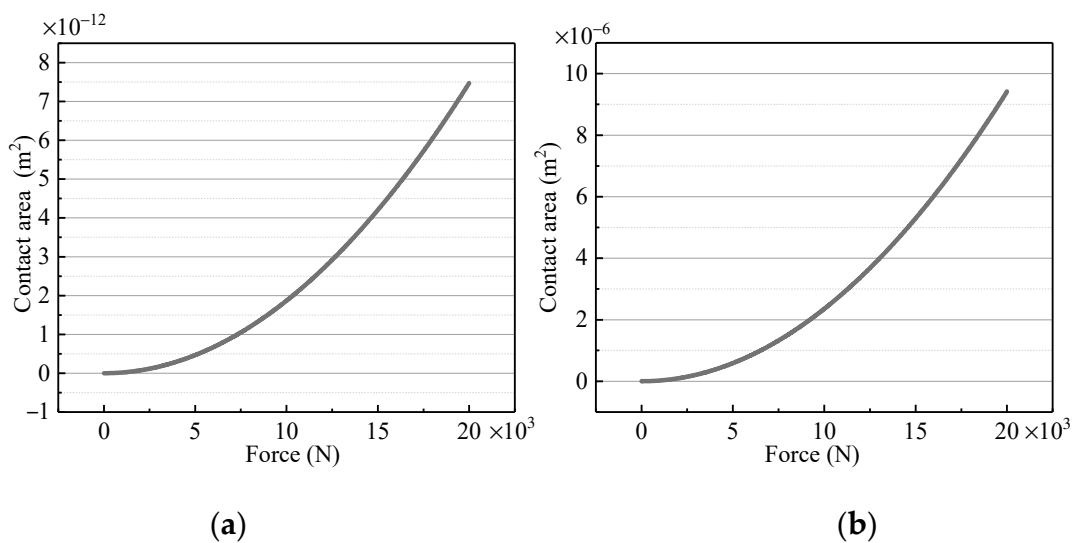


Figure 8. Change of real contact area with force. (a) Real contact area of the microconvex body. (b) Macroscopic analysis of actual contact area.

5.2. Effects of the Surface Morphology Parameters

During the operation of mechanical seals, the dynamic and static ring seal interfaces exist in a mixed lubrication state. Microconvex bodies demonstrate dynamic shear wear or adhesion failure, and the interface morphology and porosity constantly change. Some studies have shown that when the fractal dimension is small, the influence of the fractal dimension of the surface topography and the scale coefficient of the surface topography on the wear cannot be ignored.

As shown in Figure 9, the wear amount is affected by the fractal dimension D of the surface topography, for example, at 600 N and 20,000 h. The wear loss is also affected by the surface topography scale coefficient G , for example, at 600 N and 10 h. The fractal

dimension D of the surface topography shows a significant impact on the wear amount over a long time, while the scale coefficient g of surface topography has a profound impact on premature wear.

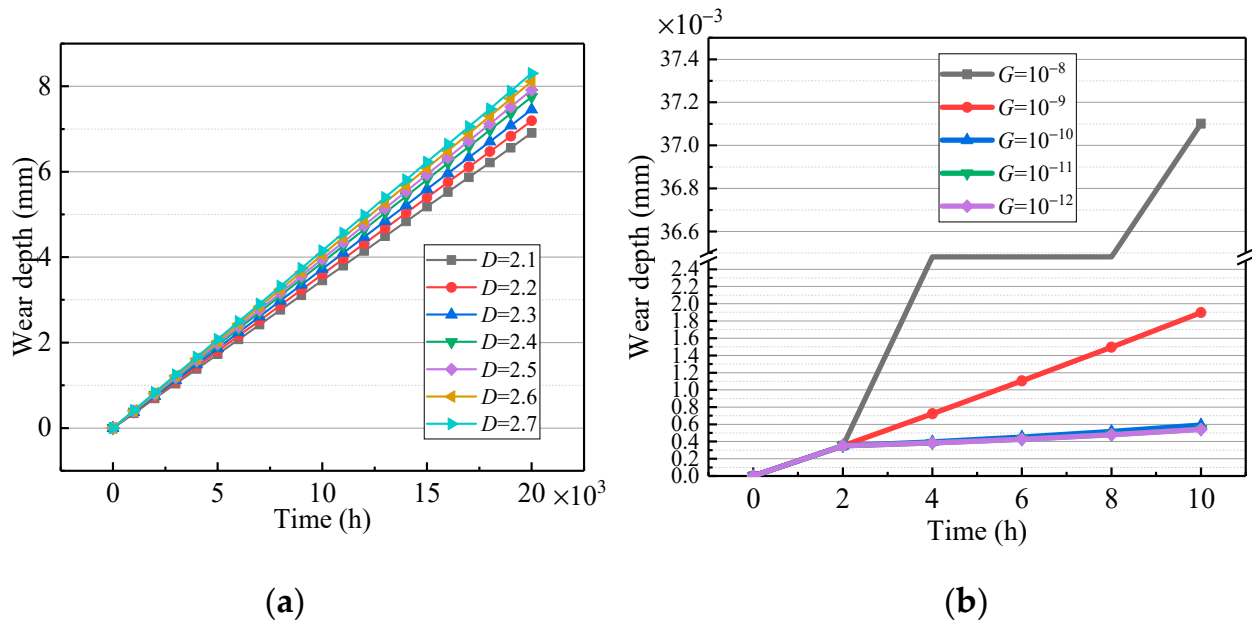


Figure 9. Influence of surface morphology parameters on wear depth. (a) Effect of fractal dimension D on wear. (b) Effect of scale coefficient G on wear.

6. Conclusions

In this study, a segmental fractal model was established for calculating the wear of a contact mechanical seal end face, and the influences of the load and fractal parameters on wear are studied. The main conclusions include:

(1) The proposed wear model (based on piecewise fractal theory) considers both the abrasive wear and the adhesive wear processes. The results closely match the experimental data, the traditional Archard model, and the M–B modified model.

(2) The increase in load engages more contact area, which increases the furrow effect and adhesion effect between solids. With the increase of the actual contact area, plastic deformation becomes dominant, and the increasing trend of the actual contact area increases the wear rate.

(3) The fractal dimension D of the surface topography has a more significant effect on the wear amount over a long time, while the scale coefficient G of surface topography has a pronounced effect on premature wear.

(4) The initial surface parameters D , G , and contact load have significant effects on the wear loss. The wear loss calculated by the model increases with an increase of specific load (in a certain range) on the end face, and its change rate shows an upward trend. It increases with an increase of the fractal dimension of the surface topography and decreases with a decrease of the scale coefficient of the surface topography.

Author Contributions: Data curation, X.N. and C.M.; formal analysis, Y.Z.; investigation, C.M.; methodology, C.M.; resources, Y.Z.; software, X.N.; supervision, J.S.; validation, C.M.; visualization, X.N. and J.S.; writing—original draft, C.M.; writing—review and editing, X.N. All authors have read and agreed to the published version of the manuscript.

Funding: This work was supported by the National Key R&D Program of China (2018YFB2000800).

Data Availability Statement: Not applicable.

Conflicts of Interest: The authors declare no conflict of interest.

Nomenclature

h	Wear thickness, mm
t_1	The running in time, s
K_s	The abrasive wear coefficient
F	The load, N
H	Hardness of the stationary ring material
K	Wear factor
v	Average slip velocity, $\text{m}\cdot\text{s}^{-1}$
ξ	Probability of generating wear debris
ϕ	Material parameter
a	Area of the microconvex body, m^2
a_1	The maximum microconvex area, m^2
a_1	The maximum area of the contact point, m^2
a_c	The critical area to distinguish elastic–plastic contact, m^2
D	Fractal dimension
G	Amplitude coefficient of fractal parameter.
L	Wavelength distance
w	The total volume of debris, m^3
P	Pressure of the sealing medium, Pa

References

- Mayer, E. *Mechanical Seal*, 6th ed.; Yao, Z., Xu, Z., Wang, J., Eds.; Chemical Industry Press: Beijing, China, 1981.
- Gu, Y. Judgment of friction state and analysis of friction characteristics of mechanical seals. *Fluid Eng.* **1991**, *5*, 9–16, 64.
- Wei, L.; Liu, Q.; Zhang, P. Sliding Friction Surface Contact Mechanics Model Based on Fractal Theory. *J. Mech Eng.* **2012**, *48*, 106–113. [[CrossRef](#)]
- Bian, W. Failure Analysis of Mechanical Seal of Main Pump in Nuclear Power Plant. *Fail. Anal. Prev.* **2021**, *16*, 134–138.
- Archard, J. Contact and rubbing of flat surfaces. *J. Appl. Phys.* **1953**, *24*, 981–988.
- Gu, Y. *Practical technology of mechanical seal*; Mechanical Industry Press: Beijing, China, 2001; pp. 143–155.
- Wei, L.; Gu, B.; Zhang, P. Wear prediction for end face of contact mechanical seals. *J. Nanjing Univ. Technol. (Nat. Sci. Ed.)* **2012**, *34*, 16–21.
- Farroni, F.; Sakhnevych, A.; Timpone, F. Physical modelling of tire wear for the analysis of the influence of thermal and frictional effects on vehicle performance. *Proc. Inst. Mech. Eng. Part L J. Mater. Des. Appl.* **2017**, *231*, 151–161. [[CrossRef](#)]
- Meruva, K.; Bi, Z.; Mueller, D.; Kang, B. Formulation and validation of multidisciplinary design problem on wear and fatigue life of lead screw actuators. *Math. Probl. Eng.* **2013**, *2013*, 303967.
- Qin, W.; Duan, L. Wear predictions for cams in line contacts based on multidisciplinary simulation. *Ind. Lubr. Tribol.* **2015**, *67*, 159–165.
- Mandelbrot, B.B. *Fractals: Form, Chance, and Dimension*; W. H. Freeman and Company: San Francisco, CA, USA, 1977.
- Majumdar, A.; Bhushan, B. Fractal model of elastic–plastic contact between rough surfaces. *Trans. ASME J. Tribol.* **1991**, *113*, 1–11. [[CrossRef](#)]
- Sun, J.; Ji, Z.; Ma, C. Reanalysis of the contact mechanics for rough surfaces. *Chin. J. Theor. Appl. Mech.* **2018**, *50*, 68–77.
- Ge, S.; Suo, S. The Computation Methods for the Fractal Dimension of Surface Profiles. *Tribology* **1997**, *17*, 66–74.
- Alben, K. Books and Software: Design, analyze, and optimize with Design-Expert. *Anal. Chem.* **2002**, *74*, 222 A–223 A.
- Ji, Z.; Sun, J.; Ma, C.; Yu, Q.; Lu, J. Key scientific problems for studying leakage mechanism of contact mechanical seal interface. *CIESC J.* **2017**, *68*, 2969–2978.
- Wang, X.; Zhang, S.; Fan, Q. Abrasive Wear Model Based on Fractal Theory. *Lubr. Seal.* **2002**, *3*, 2–4, 41.
- Liefferink, R.W.; Hsia, F.; Weber, B.; Bonn, D. Friction on Ice: How Temperature, Pressure, and Speed Control the Slipperiness of Ice. *Phys. Rev. X* **2021**, *11*, 11025.
- Bonn, D. The physics of ice skating. *Nature* **2020**, *577*, 173–174.
- Ramin, A.; Kai, Z. Micromechanics of material detachment during adhesive wear: A numerical assessment of Archard’s wear model. *Wear* **2021**, *476*, 203739.
- Yu, Q.; Sun, J.; Yu, B.; Ma, C. Experimental research on friction characteristics of contacting mechanical seal. *Exp. Technol. Manag.* **2016**, *33*, 38–41 + 44.
- Ji, Z. Research on Interfacial Leakage Mechanism of Contact Mechanical Seal Based on Percolation Theory. Ph.D. Thesis, Nanjing Forestry University, Nanjing, China, 2018.
- Prandtl, L. Ein Gedankenmodell zur kinetischen Theorie der festen Körper. *ZAMM* **1928**, *8*, 85–106.
- Zhang, T.; Wang, H.; Hu, Y. Atomic theory without wear and friction. *J. Tribol.* **2001**, *5*, 396–400.

25. Ji, Z.; Sun, J.; Lu, J.; Ma, C.; Yu, Q. Predicting method for static leakage of contacting mechanical seals interface based on percolation theory. *J. Tribol.* **2017**, *37*, 734–742.
26. Soha, B.; Pierre, A.; Siegfried, F. Explicit formulations of adhesive wear extension in fretting interfaces applying the contact oxygenation concept. *Wear* **2022**, *488–489*, 204147.

Disclaimer/Publisher’s Note: The statements, opinions and data contained in all publications are solely those of the individual author(s) and contributor(s) and not of MDPI and/or the editor(s). MDPI and/or the editor(s) disclaim responsibility for any injury to people or property resulting from any ideas, methods, instructions or products referred to in the content.